Aksaray University
Journal of Science and Engineering
e-ISSN: 2587-1277
http://dergipark.gov.tr/asujse
http://asujse.aksaray.edu.tr

Aksaray J. Sci. Eng.
Volume **4,** Issue **1,** pp. **30-42.**
doi: 10.29002/asujse.657837
Available online at DergiPark AKADEMİK

Research Article

Range Determination of the Influence of Carrier Concentration on Lattice Thermal Conductivity for Bulk Si and Nanowires

Ibrahim Nazem Qader[1,*], Botan Jawdat Abdullah[2], Mustafa Saeed Omar[2]

[1]University of Raparin, College of Science, Department of Physics, Sulaimaneyah, Iraq
[2]University of Salahaddin, College of Science, Department of Physics, Erbil, Iraq

▪*Received Date:* Dec 15, 2019 ▪*Revised Date:* Apr 27, 2020 ▪*Accepted Date:* May 05, 2020 ▪*Published Online:* Jun 21, 2020

Abstract

Mathematical modeling has been extended to simulate some physical systems to calculate some parameters that may need a sophisticated cost or may have some obstacles to be measured directly with an experimental method. In this study, the Modified Callaway Model has been used to calculate size dependence lattice thermal conductivity (LTC), and the influence of carrier concentration for bulk Si and its nanowires (NWs) with diameters of 22, 37, 56, and 115 nm has been investigated. Calculations were performed from 3K to 1600K for all cases. The effects of carrier concentration on LTC has found to begin from (10^{16} cm^{-1}) for the bulk state and that increased to (10^{24} cm^{-1}) for the NW with a diameter of 22 nm. The temperature that the maximum effect of carrier concentration can occur, has found to be at (10 K) for the bulk, and that increased to (340 K) for the (22 nm) Si NW.

Keywords

Lattice Thermal Conductivity; Si; Nanowires; Carrier Concentration; Mass Density

1.INTRODUCTION

In the last two decades, investigations of nanoscale parameters have got good attention particularly the carrier concentration effects on lattice thermal conductivity (LTC). Since it is significantly important for most nano-engineered appliances [1], it has been interested by many researchers in both theoretical and experimental methods [2-6].

[*]**Corresponding Author:** Ibrahim Nazem Qader, inqader@gmail.com +964-750-493-3789

It is well known that the scattering process is responsible for calculating LTC in solids, mainly phonon-phonon at high temperature, defects including electron-phonon scattering at the intermediate and at the lower temperature the boundary is controlling. However, the electron-phonon scattering is the list been investigated [7-9]. Li et al. [10] and Hochbaum et al. [11] experimentally investigated LTC for Si NWs and found a reduction of its values for smaller size diameters. For small size diameters, similar results have also been reported for GaN and Si NWs by Mamand et al. [12] and Qader et al. [2]. On the other hand, Liao et al. [13] proved a significant effect of carrier concentration as the electron-phonon scattering process in LTC.

In this work, we try to investigate the electron concentration-effect and electron-phonon scattering interaction at a low and intermediate temperature range of LTC in Si NWs. The modified mass density for a nanoscale is also used. The method of modified Callaway model calculations will be used for bulk Si and then applied to the nanosize wires as stated in the following method of calculations:

2. Method of Calculations

It is obviously known that in semiconductors acoustic phonons are responsible for transferring heat for temperature gradient between two points. This is due to the value of group velocity in semiconductors is bigger than the optical phonon velocity [14]. Callaway's phenomenological theory, which is progressed under the Boltzmann transport equation, is used for LTC of a semiconductor as follows [15-17]:

$$\kappa = AT^3 \int_0^{\theta_D/T} \tau_c \, J(x) \, dx \tag{1}$$

where $A = (k_B/\hbar)^3\left(k_B/(2\pi^2 v)\right)$, $J(x) = x^4 e^x (e^x - 1)^{-2}$, $x = \hbar\omega/k_B T$; also, k_B and $\hbar$ are the Boltzmann constant (1.38065×10^{-23} m$^2 \cdot$ kg $\cdot$ s$^{-2} \cdot$ K^{-1}), and reduced Planck constant (1.05457×10^{-23}J $\cdot$ s), respectively; in addition, τ_c, v , ω, θ_D, and T, respectively are, the combined phonon relaxation time, phonon group velocity, phonon angular frequency, Debye temperature, and absolute temperature.

Thermal conductivity for bulk can be anticipated by Eq. (1). Likewise, this equation can be used for calculating LTC, of thin films and NWs [18, 19]. Morelli et al. [20] and Asen-Palmer et al. [21] modified the Debye–Callaway model, by taking into account both transverse and longitudinal phonons explicitly and normal three phonon processes. The LTC has two terms $\kappa = \kappa_1 + \kappa_2$, with ($\kappa_1$) and ($\kappa_2$) are given by the relation [21, 20]:

$$\kappa = \kappa_L + 2\kappa_T \tag{2}$$

$$\kappa_L = \kappa_{L_1} + \kappa_{L_2} \tag{3a}$$

$$\kappa_T = \kappa_{T_1} + \kappa_{T_2} \tag{3b}$$

In Eq.(3a) each κ_{L_1} and κ_{L_2} are the usual Debye-Callaway terms which are given by:

$$\kappa_{L_1} = \frac{1}{3} A_L T^3 \int_0^{\theta_D^L} \tau_c^L(x)\, J(x)\, dx \tag{4}$$

$$\kappa_{L_2} = \frac{1}{3} A_L T^3 \left[\int_0^{\theta_D^L} \frac{\tau_c^L(x)}{\tau_N^L(x)}\, J(x)\, dx\right]^2 \left[\int_0^{\theta_D^L} \frac{\tau_c^L(x)}{\tau_N^L(x)\, \tau_R^L(x)}\, J(x)\, dx\right]^{-1} \tag{5}$$

Similarly, in Eq.(3b) κ_{T_1} and κ_{T_2} for the transverse phonons can be expressed as [22]:

$$\kappa_{T_1} = \tfrac{1}{3} A_T T^3 \int_0^{\theta_D^T} \tau_c^T(x)\, J(x)\, dx \tag{6}$$

$$\kappa_{T_2} = \frac{1}{3} A_T T^3 \left[\int_0^{\theta_D^T} \frac{\tau_c^T(x)}{\tau_N^T(x)}\, J(x)\, dx\right]^2 \left[\int_0^{\theta_D^T} \frac{\tau_c^T(x)}{\tau_N^T(x)\, \tau_R^T(x)}\, J(x)\, dx\right]^{-1} \tag{7}$$

where superscript and subscript, which denoted by *T* and *L*, are the transverse and longitudinal phonons, respectively; also θ_D is Debye temperature which is split to transverse and longitudinal value. The term of $A_{T(L)}$ is obtained by using the following relations [23]:

$$A_{T(L)} = \left(\frac{k_B}{\hbar}\right)^3 \frac{k_B}{2\pi^2 v_{T(L)}} \tag{8}$$

where $v_{T(L)}$ is the transverse (longitudinal) acoustic phonon group velocity.

The scattering process rates, which take into account in this study, are including, phonon–phonon (normal) scattering, $\tau_N^{L(T)}$ inharmonic interaction or three-photon Umklapp scattering, $\tau_U^{L(T)}$, phonon–impurity, $\tau_M^{L(T)}$, phonon–electron, $\tau_{ph-e}^{L(T)}$, phonon–boundary, $\tau_B^{L(T)}$, and phonon–dislocation $\tau_{DC}^{L(T)}$ scattering. All phonon scattering processes are represented as follows [4]:

$$\left(\frac{1}{\tau_C^{L(T)}}\right) = \left(\frac{1}{\tau_N^{L(T)}}\right) + \left(\frac{1}{\tau_U^{L(T)}}\right) + \left(\frac{1}{\tau_M^{L(T)}}\right) + \left(\frac{1}{\tau_B^{L(T)}}\right) + \left(\frac{1}{\tau_{ph-e}^{L(T)}}\right) + \left(\frac{1}{\tau_{DC}^{L(T)}}\right) \tag{9}$$

In Eq. (9), the umklapp scattering is divided into longitudinal and transverse modes as:

$$\left[\tau_U^{L(T)}\right]^{-1} = B_U^{L(T)} \left(\frac{k_B}{\hbar}\right)^2 x^2 T^3 e^{-\left(\theta_D^{L(T)}/3T\right)} \tag{10}$$

where $B_U^{L(T)}$ is the umklapp parameter strength for longitudinal (transverse) mode and expressed as:

$$B_U^{L(T)} = \frac{\hbar \gamma_{L(T)}^2}{M\, v_{L(T)}^2 \theta_D^{L(T)}} \tag{11}$$

where M is the average mass of an atom in the crystal, $\gamma_{L(T)}$ is the Gruneisen parameter that is handled to fitting the theoretical LTC curve with corresponding experimental data and normal phonon scattering has a significant effect for determining the peak value of the LTC [9]. The following mathematical expression can be used for calculating transverse and longitudinal modes of Debye temperature of bulk semiconductor [20]:

$$\theta_D^{L(T)} = \left(\frac{\omega_{L(T)} \pi^2}{V}\right)^{1/3} \frac{\hbar\, v_{L(T)}}{k_B} \tag{12}$$

with $\omega_{L(T)}$is longitudinal (transverse) zone-boundary phonon frequency. However, it is not a resistive process [22] and mathematically can be expressed as:

$$\left[\tau_N^{L(T)}\right]^{-1} = B_N^{L(T)} \omega^2 T^3 \tag{13}$$

where $B_N^{L(T)}$ is the normal parameter strength for longitudinal and transverse mode, which is equal to:

$$B_N^L = \frac{k_B^3 v_L^2 V}{M\hbar^3 v_L^5} \; and \; B_N^T = \frac{k_B^4 v_T^2 V}{M\hbar^3 v_T^5} \tag{14}$$

The phonon–impurity scattering rate due to the present impurity or isotopes in the crystal structure, can be calculated as [9]:

$$\left[\tau_M^{L(T)}\right]^{-1} = \left(I_{iso}^{L(T)} + I_{imp}^{L(T)}\right)\omega^4 \tag{15}$$

where $I_{iso}^{L(T)}$ is the phonon scattering due to different isotopes and for each mode is given as:

$$I_{iso}^{L(T)} = \frac{V\, \Gamma}{4\pi\, v_{L(T)}^3} \tag{16}$$

likewise, $I_{imp}^{L(T)}$ is the phonon scattering distribution due to impurity, which is expressed as:

$$I_{imp}^{L(T)} = \frac{3V^2\, \mathrm{S}^2}{\pi\, v_{L(T)}^3} N_{imp} \tag{17}$$

here S is the scattering factor, which is equal to one [24], N_{imp} is the concentration of impurity, and Γ is strength of the mass-difference scattering and can be found by:

$$\Gamma = \sum\nolimits_i c_i \left(\frac{m_i - \bar{m}}{\bar{m}}\right)^2 \tag{18}$$

where c_i is the percentage of atomic natural abundance, m_i is the atomic mass of the i^{th} isotope, $\bar{m}$ is the average atomic mass, which is equal to $\bar{m} = \sum_i c_i\, m_i$ and *V* is the lattice volume.

The phonon–boundary scattering rate for bulk is assumed self-sufficient of each frequency and temperature and expressed as $\left[\tau_b^{L(T)}(L)\right]^{-1} = v_{L(T)}/d$, where d is the effective diameter of the specimen which is found to be 3mm from the LTC fitting at low temperature. In nanocrystals, $\tau_b^{L(T)}$ depends on the group velocity and the effective diameter of the sample, L_{eff}. Also, it is independent of either temperature or frequency such that:

$$\left[\tau_b^{L(T)}(L)\right]^{-1} = \frac{v_{L(T)}}{L_{eff}} = v_{L(T)}\left(\frac{1}{L_c} + \frac{1}{L}\right) \tag{19}$$

where L is the length of the sample. For absolute temperature smaller than Debye temperature the value of L_{eff} approaches to cross-sectional dimensions, which is known as Casimir length (L_c). Furthermore, phonons scattered from grain or surface boundary of the sample, whereby, the relaxation rate for longitudinal (transverse) mode is given by [22]:

$$\left[\tau_b^{L(T)}(L,\varepsilon)\right]^{-1} = v_{L(T)}\left(\frac{1}{L_c}\frac{(1-\varepsilon)}{(1+\varepsilon)} + \frac{1}{L}\right) \tag{20}$$

The value of $1/L_{eff}$ is the specularity parameter, which depends on the frequency of phonon and the rate of surface roughness (ε). Moreover, ε has the value from the range ($0 \le \varepsilon \le 1$), with the maximum value (ε =1) represents phonon completely specular reflection and minimum value (ε =0) shows the phonon is completely diffuse from the surface.

A non-linear phonon scattering is necessary for phonon-dislocation interaction. Crystal including dislocation (linear defect) undergoes another phonon scattering process which is divided into short and long-range scattering. The short-range is similar to three-phonon Umklapp scattering, that phonons scatter on the center of the dislocation lines, as well as the long-range is scattering of phonon due to elastic strain field of dislocation lines [14]:

$$\left[\tau_{DC}^{L(T)}(x)\right]^{-1} = \eta\, N_D \frac{V_o^{4/3}}{v_{L(T)}^2}\left(\frac{k_B T}{\hbar}\right)^3 x^3 \tag{21}$$

where $\eta = 55$ is a weight factor which illustrates the mutual tendency of dislocation lines and the direction of the temperature gradient, and its value was found from an integration formula [24]. Furthermore, N_D is the density of the dislocation lines of all types that its value can be increased by increasing temperature and doped material in semiconductors. Electrons can

scatter phonons, so the rate of phonon-electron scattering for each longitudinal (transverse) mode is as follows [25]:

$$\left[\tau_{ph-e}^{L(T)}(x)\right]^{-1} = \frac{n_e E^2 x}{\rho\, v_{L(T)}^2\, \hbar} \sqrt{\frac{\pi m^* v_{L(T)}^2}{2k_B T}} \times exp\left(-\frac{m^* v_{L(T)}^2}{2k_B T} *\right) \tag{22}$$

here n_e is electron concentration density, E is deformation potential and ρ is the mass density. In this work, the modified mass density for a nanoscale is used, which is not constant as in the bulk material. Therefore, nanosize dependent mass density is calculated from the following relation [26, 27]:

$$\rho(r) = \frac{\rho(\infty)\, V(\infty)}{V(r)} \tag{23}$$

where $\rho(\infty)$ is the bulk mass density and $\rho(r)$ its nanosize dependence. The sound group velocity $v(r)$ is a nanoscale size-dependent parameter. It can be calculated as a function of nanowires diameter from the nanosize dependent of Debye temperature $\theta(r)$, according to the following [28, 29]:

$$\frac{v(r)}{v(\infty)} = \frac{\theta_D(r)}{\theta_D(\infty)} \tag{24}$$

Hence, r denoted by the nanowire radius, $v(\infty)$ and $\theta_D(\infty)$ are bulk state group velocity and the Debye temperature. $\theta_D(r)$ can be calculated from the nanosize dependence of the melting temperature $T_m(r)$ as in the following relation:

$$\left(\frac{\theta_D(r)}{\theta_D(\infty)}\right)^2 = \frac{T_m(r)}{T_m(\infty)} \tag{25}$$

where $T_m(\infty)$ is the bulk melting temperature and the $T_m(r)$ can be calculated depending on the $T_m(\infty)$ and the lattice volume nanosize dependence $V(r)$ as [30, 31]:

$$\frac{T_m(r)}{T_m(\infty)} = \left(\frac{V(r)}{V(\infty)}\right)^{2/3} \exp\left[-\frac{2(S_m(\infty) - R)}{3R\left(\frac{r}{r_c} - 1\right)}\right] \tag{26}$$

where $S_m(\infty)$ is the melting entropy, R is gas constant, r_c, it is a critical radius in which the materials melt at (0 K) and is equal to 3h, where h is the 1st surface layer high and is equal to (3.36 Å) for Si. $V(\infty)$ is the lattice volume for the bulk state of Si structure and is equal to (19.981 Å^3) while $V(r)$ is the nanosize dependent lattice volume and can be calculated from the relation $(a^3(r)/8)$, since, the unit cell structure with a nanosize lattice parameters $a(r)$ contains 8 lattices, $a(r)$ is calculated from [30]:

$$a(r) = \frac{4}{\sqrt{3}}\, d_{mean}(r) \tag{27}$$

where $d_{mean}(r)$ is the lattice mean bond length in Si NWs and can be calculated from the following relation [26]:

$$d_{mean}(r) = h - \Delta d_{mean}(r_c) \tag{28}$$

where $\Delta d_{mean}(r_c)$ is the increase in mean bond length as a function of (r) and calculated by the following relation [26]:

$$d_{mean}(r) = \Delta d_{mean}(r_c) \exp\left[\frac{-2S_m(\infty) - R}{3R\left(\frac{r}{r_c} - 1\right)}\right]^{1/2} \tag{29}$$

Hence $\Delta d_{mean}(r_c)$ is the maximum increase in the mean bond length and for Si is equal to (nm) calculation for (r), $a(r)$, and $\theta(r)$ used in the calculation for LTC in this work.

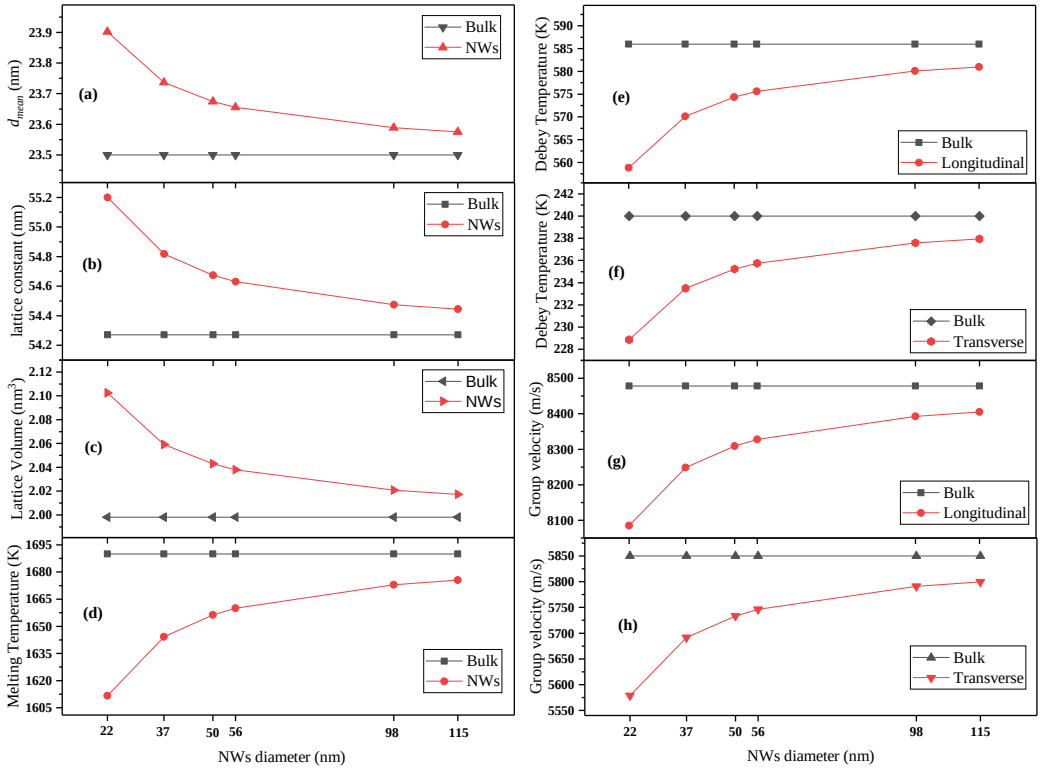

Figure 1. Diameter dependent parameters for all Si NWs. **(a)** mean bond length, **(b)** lattice constant, **(c)** lattice volume, **(d)** melting temperature, Debye temperature for **(e)** longitudinal, and **(f)** transverse, group velocity for **(g)** longitudinal, and **(h)** transverse mode.

3. Analysis of results

The parameters that obtained for fitting the calculated LTC curves to that of the experimental data by process of trial and error are listed in Table 1. These parameters are increases with the decrease of nanowires diameter, including impurities (N_{imp}), dislocation (N_D), carrier concentration (n_e), surface roughness (ε), longitudinal and transverse Grüneisen parameter (γ_L and γ_T), are affected by the decrease of NWs diameters but in nanosize systematic.

Table 1. Size dependence fitting parameters for bulk and nanowires of Si.

r (nm)	N_{imp} (m^{-3})	N_D (m^{-2})	n_e (m^{-3})	ε	γ_L	γ_T
22	8.0×10^{25}	7×10^{15}	1.9×10^{25}	0.850	0.933	0.933
37	5.6×10^{25}	4×10^{16}	5×10^{23}	0.840	0.914	0.914
56	3.3×10^{25}	3.3×10^{16}	1.7×10^{23}	0.830	0.905	0.905
115	1.1×10^{25}	1.1×10^{14}	5×10^{21}	0.475	0.896	0.896
Bulk	1.0×10^{22}	1×10^{12}	1×10^{16}		4.0	0.385

Table 2. Calculated size-dependent parameters for bulk and nanowires of Si.

r (nm)	d_{mean} (Å)	α (Å)	V (Å^3)	ρ (kg.m^{-3})	T_m (K)	θ_D^L (K)	θ_D^T (K)	v_L (m.s^{-1})	v_T (m.s^{-1})
22	2.390	5.5200	21.025	2236	1612	558.82	228.87	8084.71	5578.62
37	2.374	5.4817	20.591	2283	1644	570.12	233.50	8248.31	5691.51
56	2.366	5.4630	20.380	2306	1660	575.60	235.74	8327.59	5746.21
115	2.358	5.4445	20.174	2330	1676	580.98	237.95	8405.41	5799.91
Bulk	2.350 [c]	5.4271	19.981	2352	1685[b]	586.00[a]	240.00[c]	8478.00[a]	5850.00[a]

[a]Ref. [32], [b]Ref. [22], [c]Ref. [33]

Table 3. Constant parameters used in this work.

Parameters	***Symbols***	**Values**	**Ref.**
Weight factor	η	0.55	[9]
Average atomic mass		28·0855 (amu)	[22]
Mass per atom	M	4.7×10^{-26} (kg)	[22]
Strength of the mass-difference scattering	Γ	2.014×10^{-4}	[22]
Silicon isotopes		92.2% ^{28}Si	[22]
		4.7 % ^{29}Si	
		3.1 % ^{30}Si	
Ideal gas constant	R	8.314 $(J.K^{-1}.mol^{-1})$	[32]
First surface layer height	h	0.3368 (nm)	[32]
Enthalpy of fusion	H_m	49.819 (J.mol^{-1})	
Bulk overall melting entropy	$S_m(\infty)$	29.47×10^{-3}	[2]
		(J $K^{-1}mol^{-1}$)	
Deformation potential	E_n	9.5 (eV)	[25]
Effective mass	m^*	0.26 m_e	[34]

The obtained results including $d_{mean}(r)$, $a(r)$, $V(r)$ increases with the decrease of nano-wire diameter while other parameters such as $\rho(r)$, $T_m(r)$, longitudinal and transverse Debye

temperature $\theta_D^L(r)$ and $\theta_D^T(r)$, as well as both longitudinal and transverse group velocity $v_D^L(r)$ and $v_D^T(r)$ are decreases with the reduction of size (Table 2). Fig. 1 shows the size-dependent values for all calculated parameters and LTC values as they obtained by using the data listed in Table 1 and Table 2 for Bulk Si and its NWs of diameters 22 nm, 37 nm, 56 nm, and 115 nm.

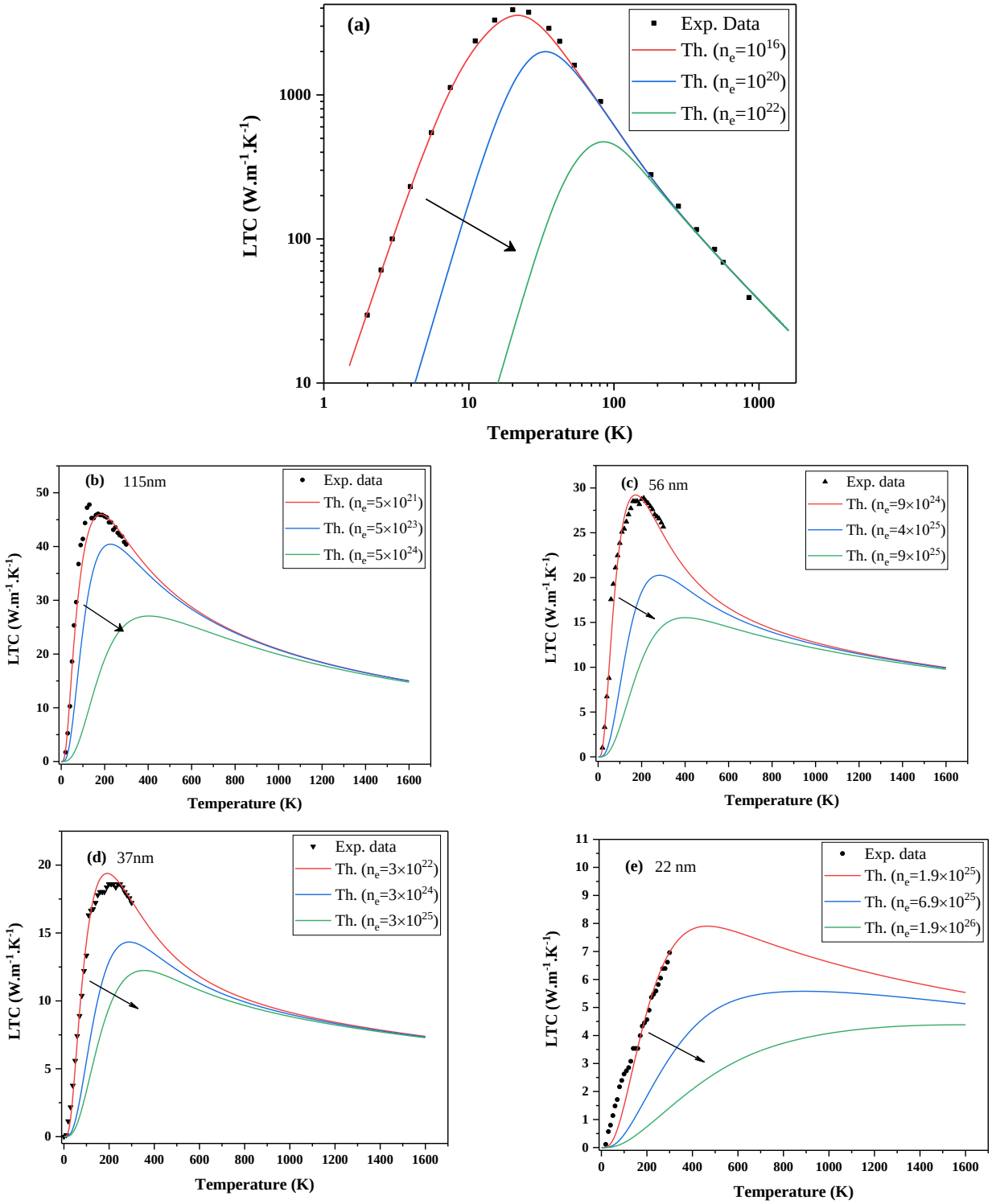

Figure 2. Diameter dependent parameters for all Si NWs. **(a)** mean bond length, **(b)** lattice constant, **(c)** lattice volume, **(d)** melting temperature, Debye temperature for **(e)** longitudinal and **(f)** transverse, group velocity for **(g)** longitudinal and **(h)** transverse mode.

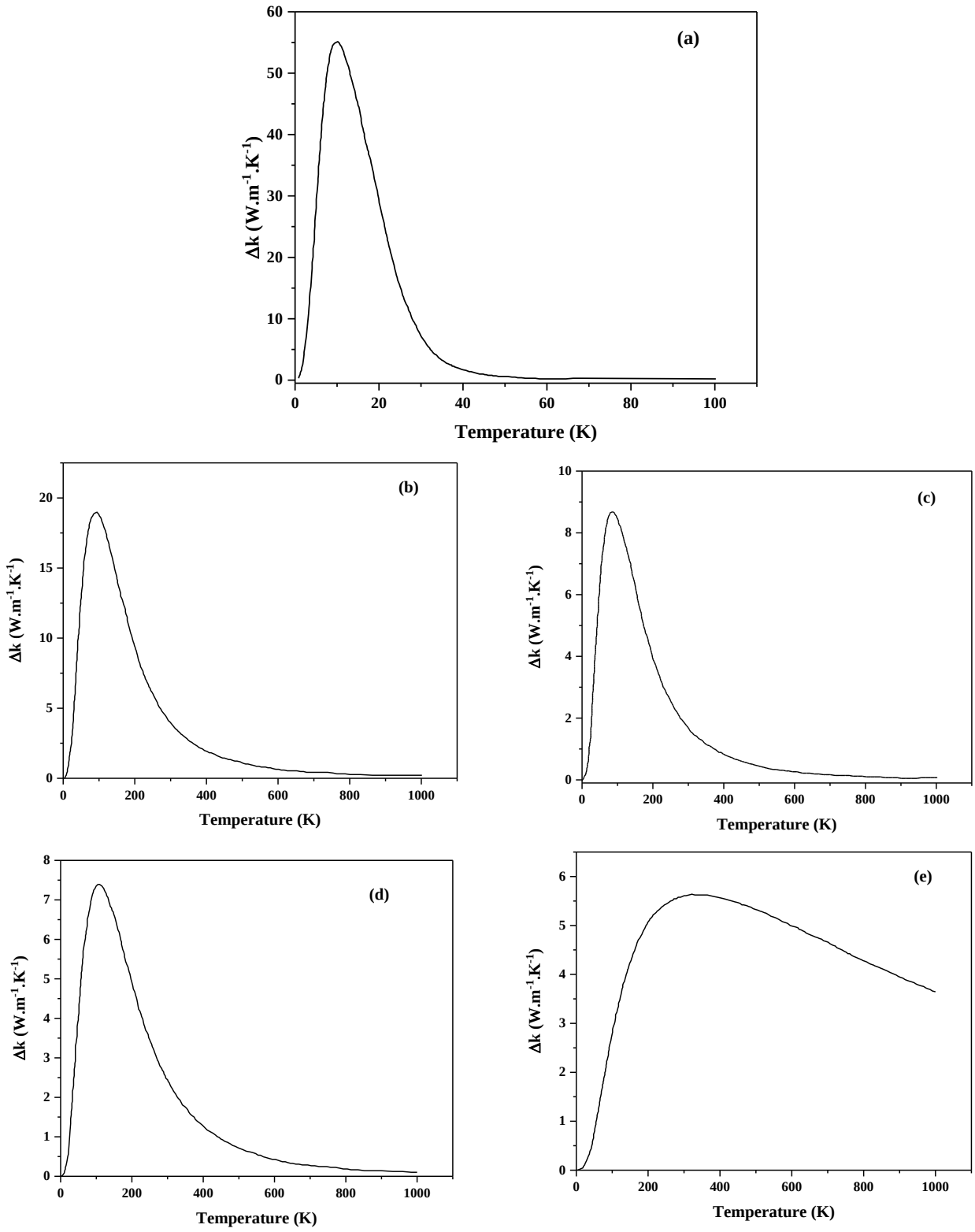

Figure 3. The change in LTC ($\Delta\kappa$) vs. temperature for **(a)** bulk Si and NWs with diameters of **(b)** 115nm, **(c)** 56nm, **(d)** 37nm, and **(e)** 22nm. $\Delta\kappa$ is obtained by subtracting fitted LTC with its obtained values when carrier concentration changed in the step of 10^2.

For the bulk Si, Eqs. (1) to (22) were used with the bulk parameters that are tabulated in Table 3. For nanowires, the nanosize dependence of mass density, group velocity, Debye temperature, melting point, and mean bond length values were calculated through Eqs. (23) to (27). The

recalculations temperature dependence of LTC with different electron concentration n_e is shown in Fig. 2. In general and as expected, the increase of n_e will decrease LTC, that's since an electron-phonon scattering, which shows the decrease of LTC as a function of temperature, it looks the maximum effects have occurred at temperature 10 K in bulk Si and 91, 86, 107 and 333 K in Si nanowires with diameters of 55, 37, and 22 nm, respectively. According to the results, the effects of carrier concentration decreased by decreasing the diameter of Si nanowire. The temperature where $n_e$shows its maximum effect were also investigated. The results are shown in Fig. 3. This temperature strongly depends on the type of material and the diameter of the nanowire.

4.Conclusions

Modified Callaway Model was used to fit theoretical LTC with experimental data for Si bulk and NWs in the range of 3K to 1600K. For calculating LTC some size-dependent parameters were obtained, including mean bond length, the lattice constant, lattice volume, melting temperature, Debye temperature, and group velocity for each longitudinal and transverse mode. The effect of carrier concentration on LTC starts from 10^{16} for the bulk Si, these values increase dramatically to about 10^{22} for a nanowire solid. By increasing carrier concentration, LTC curves shifted to the higher temperature, whereas there is no any change determined in the intermediate temperature (LTC peak) and high-temperature region

Acknowledgment

Authors would like to acknowledge University of Raparin and Salahaddin University-Erbil under grand number (7/29/2359-2472017) for their financial support.

References

[1] M. Omar, Structural and Thermal Properties of Elementary and Binary Tetrahedral Semiconductor Nanoparticles, Int J Thermophys 37(1) (**2016**) 11. doi:10.1007/s10765-015-2026-9.

[2] I. N. Qader, M. Omar, Carrier concentration effect and other structure-related parameters on lattice thermal conductivity of Si nanowires, Bull Mater Sci 40(3) (**2017**) 599-607. doi:10.1007/s12034-017-1393-1.

[3] N.-W. Park, W.-Y. Lee, J.-A. Kim, K. Song, H. Lim, W.-D. Kim et al., Reduced temperature-dependent thermal conductivity of magnetite thin films by controlling film thickness, Nanoscale research letters 9(1) (**2014**) 96. doi:10.1186/1556-276X-9-96.

[4] I. N. Qader, B. J. Abdullah, H. H. Karim, Lattice Thermal Conductivity of Wurtzite Bulk and Zinc Blende CdSe Nanowires and Nanoplayer, Eurasian Journal of Science & Engineering 3(1) (**2017**) 9-26. doi:10.23918/eajse.v3i1sip9.

[5] J. Kang, J. W. Roh, W. Shim, J. Ham, J. S. Noh, W. Lee, Reduction of Lattice Thermal Conductivity in Single Bi-Te Core/Shell Nanowires with Rough Interface, Adv Mater 23(30) (**2011**) 3414-9. doi:10.1002/adma.201101460.

[6] M. Omar, H. Taha, Effects of nanoscale size dependent parameters on lattice thermal conductivity in Si nanowire, Sadhana 35(2) (**2010**) 177-93. doi:10.1007/s12046-010-0019-8.

[7] J. Vandersande, C. Wood, The thermal conductivity of insulators and semiconductors, Contemporary Physics 27(2) (**1986**) 117-44.

[8] B. K. Agrawal, G. Verma, Lattice thermal conductivity at low temperatures, Phys Rev 126(1) (**1962**) 24. doi:10.1103/PhysRev.126.24.

[9] S. M. Mamand, M. S. Omar, A. J. Muhammad, Nanoscale size dependence parameters on lattice thermal conductivity of Wurtzite GaN nanowires, Materials Research Bulletin 47(5) (**2012**) 1264-72.

[10] D. Li, Y. Wu, P. Kim, L. Shi, P. Yang, A. Majumdar, Thermal conductivity of individual silicon nanowires, Appl Phys Lett 83(14) (**2003**) 2934-6. doi:10.1063/1.1616981.

[11] A. I. Hochbaum, R. Chen, R. D. Delgado, W. Liang, E. C. Garnett, M. Najarian, A. Majumdar and P. Yang, Enhanced thermoelectric performance of rough silicon nanowires, Nature 451(7175) (**2008**) 163-7. doi:10.1038/nature06381.

[12] S. Mamand, M. Omar, A. Muhammad, Nanoscale size dependence parameters on lattice thermal conductivity of Wurtzite GaN nanowires, Mater Res Bull 47(5) (**2012**) 1264-72. doi:10.1016/j.materresbull.2011.12.025.

[13] B. Liao, B. Qiu, J. Zhou, S. Huberman, K. Esfarjani, G. Chen, Significant reduction of lattice thermal conductivity by the electron-phonon interaction in silicon with high carrier concentrations: A first-principles study, Physical review letters 114(11) (**2015**) 115901.

[14] J. Zou, Lattice thermal conductivity of freestanding gallium nitride nanowires, Journal of Applied Physics 108(3) (**2010**) 034324.

[15] J. Callaway, Model for lattice thermal conductivity at low temperatures, Physical Review 113(4) (**1959**) 1046.

[16] M.-J. Huang, W.-Y. Chong, T.-M. Chang, The lattice thermal conductivity of a semiconductor nanowire, Journal of applied physics 99(11) (**2006**) 114318.

[17] T. M. Tritt. Thermal conductivity: theory, properties, and applications. Springer Science & Business Media; 2005.

[18] A. Balandin, K. L. Wang, Significant decrease of the lattice thermal conductivity due to phonon confinement in a free-standing semiconductor quantum well, Physical Review B 58(3) (**1998**) 1544.

[19] A. Khitun, A. Balandin, K. Wang, Modification of the lattice thermal conductivity in silicon quantum wires due to spatial confinement of acoustic phonons, Superlattices and microstructures 26(3) (**1999**) 181-93.

[20] D. Morelli, J. Heremans, G. Slack, Estimation of the isotope effect on the lattice thermal conductivity of group IV and group III-V semiconductors, Physical Review B 66(19) (**2002**) 195304.

[21] M. Asen-Palmer, K. Bartkowski, E. Gmelin, M. Cardona, A. Zhernov, A. Inyushkin, A. Taldenkov, V. I. Ozhogin, K. M. Itoh, and E. E. Haller, Thermal conductivity of

germanium crystals with different isotopic compositions, Physical Review B 56(15) (**1997**) 9431.

[22] M. S. Omar, H. T. Taha, Effects of nanoscale size dependent parameters on lattice thermal conductivity in Si nanowire, Sadhana 35(2) (**2010**) 177-93.

[23] I. N. Qader, B. J. Abdullah, M. A. Hassan, P. H. Mahmood, Influence of the Size Reduction on the Thermal Conductivity of Bismuth Nanowires, Eurasian Journal of Science & Engineering 4(3) (**2019**) 55-65. doi:10.23918/eajse.v4i3sip55.

[24] P. Klemens, The scattering of low-frequency lattice waves by static imperfections, Proceedings of the Physical Society Section A 68(12) (**1955**) 1113.

[25] J. Zou, A. Balandin, Phonon heat conduction in a semiconductor nanowire, Journal of Applied Physics 89(5) (**2001**) 2932-8.

[26] B. J. Abdullah, Q. Jiang, M. S. Omar, Effects of size on mass density and its influence on mechanical and thermal properties of ZrO2 nanoparticles in different structures, Bulletin of Materials Science 39(5) (**2016**) 1295-302.

[27] B. J. Abdullah, M. S. Omar, Q. Jiang, Size dependence of the bulk modulus of Si nanocrystals, Sādhanā 43(11) (**2018**) 174.

[28] L. Liang, B. Li, Size-dependent thermal conductivity of nanoscale semiconducting systems, Physical Review B 73(15) (**2006**) 153303.

[29] J. Dash, History of the search for continuous melting, Reviews of Modern Physics 71(5) (**1999**) 1737.

[30] M. S. Omar, Models for mean bonding length, melting point and lattice thermal expansion of nanoparticle materials, Materials Research Bulletin 47(11) (**2012**) 3518-22.

[31] B. J. Abdullah, M. S. Omar, Q. Jiang, Size effects on cohesive energy, Debye temperature and lattice heat capacity from first-principles calculations of Sn nanoparticles, Proceedings of the National Academy of Sciences, India Section A: Physical Sciences 88(4) (**2018**) 629-32.

[32] M. S. Omar, Structural and Thermal Properties of Elementary and Binary Tetrahedral Semiconductor Nanoparticles, International Journal of Thermophysics 37(1) (**2016**) 11.

[33] M. S. Omar, Lattice thermal expansion for normal tetrahedral compound semiconductors, Materials research bulletin 42(2) (**2007**) 319-26.

[34] V. Pudalov, M. Gershenson, H. Kojima, N. Butch, E. Dizhur, G. Brunthaler, A. Prinz, and G. Bauer, Low-density spin susceptibility and effective mass of mobile electrons in Si inversion layers, Physical Review Letters 88(19) (**2002**) 196404.